Vibration Analysis of Post-buckled Fluid-conveying Functionally Graded Pipe

Abdellatif Selmi (selmi_fr2016@yahoo.com)
Prince Sattam bin Abdulaziz University

Research

Keywords: Post-buckling, Exact solution, Vibration, Fluid-conveying pipe, Functionally graded material

Posted Date: December 28th, 2020

DOI: https://doi.org/10.21203/rs.3.rs-122825/v1

Vibration analysis of Postbuckled fluid-conveying functionally graded pipe

Abdellatif Selmi[1,2,*]

[1]Prince Sattam bin Abdulaziz University, College of Engineering, Civil Engineering Department, Alkharj, Saudi Arabia

[2]University of Tunis El Manar, National Engineering School of Tunis, Civil Engineering Laboratory, Tunis, Tunisia.

*Corresponding author:

Prince Sattam bin Abdulaziz University, College of Engineering, Civil Engineering Department, Alkharj, Saudi Arabia

Email: Selmi-fr2016@yahoo.com

Abstract

The vibration of post-buckled fluid-conveying pipe made of functionally graded material is analyzed. The pipe material properties are assumed to be graded in the thickness direction according to power-law distribution. An exact solution is obtained for the post-buckling deformation of the fluid-conveying functionally graded pipe with various boundary conditions. The linear vibration problem is solved around the first buckled configuration and the natural frequencies of the three lowest vibration modes are obtained. The influences of power-law exponent, initial tension, fluid density and fluid velocity on the static deflection and free vibration frequencies are studied.

Keywords: Post-buckling, Exact solution, Vibration, Fluid-conveying pipe, Functionally graded material.

1. Introduction

Fluid-conveying pipes have many industrial applications, especially in power transmission, petrochemical, marine, ocean thermal energy conversion, nuclear and oil industries. The use of classical material made pipes may face limitations like excessive vibration and noise. To suppress the excessive vibration and to avoid failure due to large motions of pipes conveying fluid, the dynamic characteristics of fluid-conveying pipes have been studied substantially and is still of interest today [1-8].

The first studies [9] focused on linear free vibrations with piping stability. Experimental, numerical and analytical techniques were developed and used to study the dynamic of pipe-fluid interactions. The generalized integral transform technique was adopted by An and Su [10] to analyze the dynamic behavior of pipes conveying liquid-gas. They demonstrate that the gas content has important effects on the frequencies and vibration amplitudes of the pipes.

The stability of fluid-conveying pipes composed of two different materials was investigated by Dai and Wang [11]. The significant impact of high flow velocities on the piping system stability was demonstrated. The dynamics of a fluid-conveying pipe under a moving sprung mass was investigated by Sadeghi and Karimi-Dona [12] based on finite-element and state-space algorithms. It was proved that the moving mass velocity and the natural frequency are inversely proportional. Experimental and theoretical methods were used by Wang et al. [13-14] to explore the change and the stability of cantilevered pipes having conical shape. Yang et al. [15] applied multi-scale method in order to study the stability of a simply supported pipe conveying pulsatile flow in subharmonic and combination resonances. Panda and Kar [16] used a numerical method to examine the stability, buckling configuration and vibration response of a hinged pipe. Seo et al. [17] developed a finite-element formulation to investigate the stability and forced vibration of fluid-conveying pipes with pulsatile flow. Zhai et al. [18] developed the deflection equation for Timoshenko curved pipes conveying fluid using Hamilton's principle and applied the pseudo-excitation method to discuss dynamic responses under the condition of random excitation. The stability of a pinned pipe under thermal loads was studied by Qian and Wang [19] using the differential quadrature method. Applying Galerkin and finite-difference methods, Chang and Modarres-Sadeghi [20] examined the dynamics of a pipe under a base excitation. The dynamic instability of a pipe caused by the internal fluid flows with pulsatile flow velocity is usually known by a parametric instability region in the two-dimensional domain of frequency and fluid velocity amplitude [21-28]. The pre-buckled state is characterized by periodic or quasi-periodic oscillation of the pipe. However, the post-buckling state of fluid conveying pipe may leads to chaotic motion of the pipe [28-30]. The monitor of parameters technique [31] and the active control approach [32] are recommended to get rid of the excessive vibration and defeat due to large motions of pipes conveying fluid.

The shortcoming due to the instability of the isotropic and homogeneous pipe which occurs at a low flow velocity of the internal fluid [33] can be mitigated using functionally graded (FG) pipes. Unlike the dynamics of fluid-conveying pipes made of conventional isotropic material structures which has been investigated widely in the literature, researches on the postbuckling behavior of FG piping system are limited. FGM are a mixture of two or more constituent materials whose volume fractions vary smoothly and continuously along a preferred direction [34, 35]. In the investigations reported in [36, 37], the linear vibration of fluid-conveying FG pipes has been performed. It is found that the stability of fluid-conveying pipes is improved considerably when the pipes are made of FGM instead of conventional isotropic material. In fact, the improved stability of a FG pipe arises mainly because of its high stiffness. Deng et al. [38] analyzed the instability of a multi-span viscoelastic pipe made of FGM using the wave-propagation approach and reverberation-ray matrix algorithm. Wang and Liu [39] used a symplectic approach to assess the impact of the power-law exponent on the deflection and stability of a clamped FG pipe. By utilizing the generalized integral transform method, An and Su [40] analyzed the linear vibration and amplitudes of a functionally graded pipe conveying fluid. Hosseini and Fazelzadeh [36] considered a cantilever FG pipe operating in the thermal environment and studied its thermo-mechanical stability for the internal fluid flow with the steady flow velocity. Eftekhari and Hosseini [37] carried out a similar study for investigating the stability of a rotating FG pipe.

In the mentioned researches, only the buckling analysis of fluid-conveying functionally graded pipe is investigated, and the post-buckling analysis has been neglected. To the best of the authors' knowledge, no research has been carried out on finding exact solution for the post-buckling and vibration analyses of FG fluid-conveying functionally graded pipe with different boundary conditions. This work therefore aimed to present a closed-form solution for the post-buckling configuration of fluid-conveying functionally graded pipe. FG fluid-

conveying functionally graded pipe is modeled based on Euler-Bernouilli beam theory. The material properties are assumed to be graded in the thickness direction according to the power-law distribution. Free vibration of the beam in the vicinity of the buckled configuration is also investigated. Effects of different control parameters, such as the power law index, flow velocity, fluid density and initial tension on the critical flow velocities and post-buckling behavior are highlighted.

2. Problem formulation

Figure 1 shows a fluid-conveying FGM pipe. The fluid is considered traveling at a flow velocity, V. The internal and external radius and the length of FG pipe are denoted by r_i, r_0 and L, respectively.

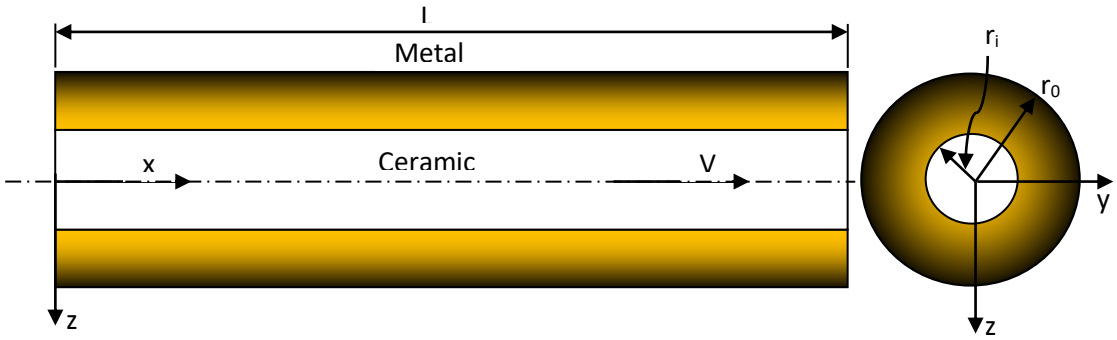

Fig. 1. Schematic representation of a FG pipe conveying fluid

The material properties of the FG pipe vary across its thickness according to a power-law distribution as:

$$E(r) = V_i E_i + V_0 E_0 \tag{1}$$

$$\rho(r) = V_i \rho_i + V_0 \rho_0 \tag{2}$$

with $V_i = \left(\frac{r_0 - r}{r_0 - r_i} \right)^n$ and $V_0 = 1 - V_i$

where E(r) and ρ(r) are the Young's modulus and the mass density of the FG pipe, respectively. E_i and E_0 represent the material properties in the outer and inner layers,

respectively. V_i and V_0 denote the volume fractions of the ceramic and metal. n is the power-law exponent.

According to the Euler-Bernoulli theory and based on the Hamilton principle, the governing equation of transverse oscillation for the FG pipe is derived by Tang et al. (2018) as follow:

$$\left(m_f + m_p\right)\frac{\partial^2 \bar{w}}{\partial t^2} + 2m_f v\frac{\partial^2 \bar{w}}{\partial t \partial \bar{x}} + \left(m_f V^2 - p_0\right)\frac{\partial^2 \bar{w}}{\partial \bar{x}^2} + EI^*\frac{\partial^4 \bar{w}}{\partial \bar{x}^4} - \frac{EA^*}{2L}\frac{\partial^2 \bar{w}}{\partial \bar{x}^2}\int_0^L\left(\frac{\partial \bar{w}}{\partial \bar{x}}\right)^2 d\bar{x} = 0 \qquad (3)$$

where p_0 stands for the initial axial tension and:

$$EI^* = \int_0^{2\pi}\int_{r_i}^{r_0} E(r)r^2\sin^2(\theta)rdrd\theta E(r) \qquad (4)$$

$$EA^* = \int_0^{2\pi}\int_{r_i}^{r_0} E(r)rdrd\theta E(r) \qquad (5)$$

m_f and m_p denote the mass per unit length of the fluid and the pipe, respectively; they are expressed as:

$$\begin{cases} m_f = \rho_f A_f \\ m_p = \int_A \rho(r)dA \end{cases} \qquad (6)$$

where ρ_f is the fluid mass density and A_f is the cross the flow sectional area.

The equation of motion of FG pipe conveying fluid presents a cubic-nonlinearity and is similar to the governing equation of a beam made of isotropic material.

For simplicity, the following nondimensional variables are used:

$$x = \frac{\bar{x}}{L},\quad w = \frac{\bar{w}}{r},\quad \bar{P} = m_f V^2 - p_0 \text{ and } P = \frac{\bar{P}L^2}{EI^*} \qquad (7)$$

where $r = \frac{EI^*}{EA^*}$ is the radius of gyration of the cross section. As a result, Eq. (3) is rewritten as:

$$\ddot{w} + w^{(4)} + Pw'' - \frac{1}{2}w''\int_0^1 w'^2 dx = 0 \qquad (8)$$

where the dot stands for the derivative according to time t, the prime indicates the derivative with respect to the spatial coordinate x.

The boundary conditions are:

$$\begin{aligned} &w = 0 \text{ and } w' = 0 \text{ at } x = 0 \text{ , } 1 \quad \text{for F - F pipes} \\ &w = 0 \text{ , } w' = 0 \text{ at } x = 0 \text{ and } w = 0 \text{ , } w'' = 0 \text{ at } x = 0 \quad \text{for F - H pipes} \\ &w = 0 \text{ and } w'' = 0 \text{ at } x = 0 \text{ , } 1 \text{ for H - H pipes} \end{aligned} \tag{9}$$

3. Buckling configurations

The buckling equation for a FG pipe can be obtained from Eq. (8) by eliminating the nonlinear and inertia forcing terms as:

$$w^{(4)} + Pw'' - \frac{1}{2} w'' \int_0^1 w'^2 dx = 0 \tag{10}$$

Applying the corresponding boundary conditions, the exact solutions of the nonlinear buckling problem for the buckled configurations are obtained. The reader is referred to Nayfeh and Emam [41] for the details. The exact solutions of fluid conveying FG pipe are obtained as follow:

For F-F boundary conditions

$$w(x) = c\left[1 - \frac{\lambda - \cos\lambda}{\lambda - \sin\lambda} x - \cos(\lambda x) - \frac{1 - \cos\lambda}{\lambda - \sin\lambda} \sin(\lambda x)\right] \tag{11}$$

For F-H boundary conditions

$$w(x) = c\left[1 - x - \cos(\lambda x) + \frac{\sin(\lambda x)}{\sin\lambda}\right] \tag{12}$$

For H-H boundary conditions

$$w(x) = c \sin(\lambda x) \tag{13}$$

λ^2 has the dimension of a load and is given by:

$$\lambda^2 = P - \Gamma \text{ and } \Gamma = \frac{1}{2} \int_0^1 w'^2 dx \tag{14}$$

and c is a constant expressed as:

$$c = \pm 2\sqrt{\frac{p}{\lambda^2} - 1} \tag{15}$$

The characteristic equation for λ of pipes with F-F, F-H, and H-H boundary conditions are respectively formulated as:

$$2 - 2\cos\lambda - \lambda\sin\lambda = 0 \tag{16}$$

$$\sin\lambda - \lambda\cos\lambda = 0 \tag{17}$$

$$\sin\lambda = 0 \tag{18}$$

It is obvious that the amplitude, c, of a buckling mode can exist only when P exceeds the critical buckling load of that mode.

Next, the consequences of the changes in the control parameters; fluid velocity, fluid density and initial tension on the buckled configuration of FG pipe conveying fluid for different boundary conditions (F-F, F-H and H-H) are examined. The geometrical characteristics of the FG pipe are: pipe length L = 10 m; internal radius r_i=0.08m; external radius r_o=0.1 m, respectively. The Young's modulus, Poisson's ratio, and the mass density of the FG pipe as well as the fluid mass density are set to: E_i = 151 GPa, E_o=70 GPa, ρ_i=3000 kg/m^3, ρ_o=2700 kg/m^3. Moreover, in the following section the power law gradient index is assumed n=1.

4. Effect of the control parameters on the buckled configuration

a. Effect of the fluid velocity

Under the three types of boundary conditions, Figures 2a, 3a and 4a illustrate the evolution of the dimensionless transverse displacement of the FG pipe at x= 0.25 as a function of the speed of the flowing fluid for the first three buckling modes. The fluid density and the initial tension are taken equal to p_f=1000Kg/m^3 and p_0=-20N, respectively. It is seen that the transverse displacements are zero until a certain fluid velocity (V=307.7m/s, V=220.7m/s and V=153.8m/s for F-F, F-H and H-H, respectively). At this critical point which corresponds to the first buckling, instability takes place via a branch point bifurcation, causing deflection

displacements to rise suddenly. Beyond this point, two possible stable solutions and one unstable solution for the transverse displacement can be seen. As the fluid velocity is increased beyond critical value (V=441.5m/s, V=381.1m/s, 307.7m/s for F-F, F-H and H-H, respectively) which corresponds to the second critical buckling, the pipe has three equilibria: the straight configuration, which is unstable, and two others corresponding to the first and second buckled configurations. As the fluid velocity is increased beyond the third critical buckling value, (V=618.7m/s, V=538.5m/s, V=454.8m/s for F-F, F-H and H-H, respectively), the pipe exposes three nontrivial equilibria assiciated to the three buckled configurations. As can be seen the magnitudes of the fluid velocity corresponding to the first three buckling modes depends on the boundary conditions. The higher and lower magnitudes correspond to the F-F and H-H boundary conditions which means that the higher and lower stability of a FG pipe are obtained for F-F and H-H boundary conditions, respectively. It is, also, remarkable that when fluid velocity is increased, the transverse displacement of H-H FG pipe increases more rapidly than that corresponding to the other boundary conditions.

b. Effect of the fluid density

To demonstrate the impact of the fluid density on the bifurcation diagrams of the fluid conveying FG pipe, the variation of the transverse deflection with the flow density is depicted in Figs. 2b, 3b and 4b. In this subsection V=200m/s and p_0=-20N. It is seen that the deflections are null prior to a certain fluid density (p_f = 2370 kg/m3, p_f =1211 kg/m3 and p_f =627 kg/m^3 for F-F, F-H and H-H, respectively). At this critical point, a buckling instability takes place causing transverse displacements to increase suddenly. After this point, there are two possible stable solutions and one unstable solution for the transverse displacement. The three fluid density values corresponding to the second and third buckled modes for F-F, F-H and H-H boundary conditions are respectively (p_f =4933 kg/m3, p_f =3634 kg/m3 and p_f =2438 kg/m3) and (p_f =9639 kg/m^3, p_f =7251 kg/m^3 and p_f =5425 kg/m^3). As shown, the critical

fluid density corresponding to the buckling of the FG pipe depends to the boundary conditions. The higher and lower values correspond to the F-F and H-H boundary conditions which implies that the higher and lower stability of a FG pipe are obtained for F-F and H-H boundary conditions, respectively. Moreover, it is found that the lateral deflection of the FG pipe increases when increasing the fluid density. The highest increase corresponds to H-H supports.

c. Effect of the initial tension

The bifurcation diagrams for the first three buckled modes of F-F, F-H and H-H FG pipes conveying fluid at x=0.25 are plotted against the initial tension in Figs 2c, 3c and 4c. The fluid velocity and density are V=200m/s and p_f=1000kg/m3, respectively. It is noted that as the initial tension reaches the first critical value, the undeflected position becomes unstable. Beyond this critical load, the straight configuration becomes instable and the beam gains other stable equilibrium positions, which are known as the buckled configurations. Similar tendencies are obtained for the higher buckling modes. As the axial load is increased after the second critical buckling the beam has three equilibria. As the axial load continue to increase beyond the third critical buckling load, the pipe exhibits three nontrivial equilibria corresponding to the three buckled configurations. As can be noted, the nondimensional deflection increases as p_0 increases. An important point concluded here is that the difference between the initial tensions corresponding to the buckling differs from a boundary condition to another. The most prominent is the case of F-F boundary condition.

5. Effect of power-law exponent

For various boundary conditions, the bifurcation diagrams of buckling behavior of the FGM pipe conveying fluid for various power-law exponents are investigated in this section.

The variation of the nondimensional transverse displacement against the fluid velocity, fluid density and initial tension for the first buckled configuration of a FG pipe is depicted in Figs 5-7. Results are shown for different power-law indexes. The significant impact of the power law index on the critical values of the control parameters is clearly seen. The FG pipe presented a stable and undeformed static equilibrium state for lower values of the considered control parameter. However, when the value of the parameter exceeded a certain limit, the pipe exhibited a bi-stable configuration and post-buckling after undergoing a divergence pitchfork bifurcation. Additionally, it appears from Figs. 5-7 that the post-buckling displacement of the FG pipe increased when increasing the power-law exponent, n, from one to infinity. It is remarkable that a change in the power law index affects highly the buckling values and the resulting post-buckling response which indicates that one can get a desired response just by controlling the power law index value. Higher values of the power law index lead to a significant reduction in the control parameters associated with the instability of the pipe. It implies that as the power law index increases, the pipe buckles at lower magnitudes of control parameters. In fact, a greater stiffness increases the buckling capacity of the pipe. The critical values of the control parameters corresponding to the F-F boundary conditions are the most amongst the three previously mentioned end conditions which clarify the high stability of a FG beam with fixes supports.

6. Free vibration in the post-buckling state

To study the vibration behavior in the post-buckling state, the vibrations occurs around a buckled configuration derived in the previous section is considered. To this purpose, the deflection is assumed to be in the form:

$$W(x,t) = w(x) + v(x,t) \tag{19}$$

with v(x, t) is a small dynamic disturbance around the buckled configuration w(x).

The substitution of Eq. (19) into Eqs. (8) and (9), results in:

$$\ddot{v} + v^{(4)} + \lambda^2 v'' = w'' \int_0^1 w'v'dx + \frac{1}{2} w'' \int_0^1 v'^2 dx + v'' \int_0^1 w'v'dx + \frac{1}{2} v'' \int_0^1 v'^2 dx \tag{20}$$

The governing equation of linear vibration can be derived by eliminating the nonlinear terms from Eq. (20):

$$\ddot{v} + v^{(4)} + \lambda^2 v'' = w'' \int_0^1 w'v'dx \tag{21}$$

Assume the dynamic response to be harmonic:

$$v(x) = \Phi(x) e^{i\omega t} \tag{22}$$

where $\Phi(x)$ is a linear vibration mode shape and ω is its associated natural frequency. A complete solution for the free vibration in the post-buckling state can be found in the reference [41]. The mode shape is formulated as:

$$\Phi(x) = \Phi_h(x) + \Phi_p(x) \tag{23}$$

The homogenous solution is given by:

$$\Phi_h(x) = C_1 \sin(s_1 x) + C_2 \cos(s_1 x) + C_3 \sinh(s_2 x) + C_4 \cosh(s_2 x) \tag{24}$$

and the particular solution is assumed as:

$$\Phi_p(x) = C_5 W^{"} \tag{25}$$

Where

$$s_{1,2} = \left(\pm \frac{\lambda^2}{2} + \frac{1}{2} \sqrt{\lambda^4 + 4\omega^2} \right)^{0.5} \tag{26}$$

and C_i are constants.

The solution given by Eq. (23) has to satisfy the Eq. (21) which results in:

$$C_5 \left(W^{(4)} + \lambda^2 W^{(4)} \right) - C_5 \omega^2 W'' = W'' \Lambda + C_5 \int_0^1 W'W'''dx \tag{27}$$

where $\Lambda = \int_0^1 w'\Phi_h' dx$ (28)

With the aid of Eq. (10), Eq. (27) leads to:

$$\Lambda + C_5\left(\omega^2 + \int_0^1 W'W''' dx\right) = 0 \quad (29)$$

From the solution of Eq. (23) with the boundary conditions given by Eq. (9), a system of four algebraic equations for the constants C_i is built up. Based on Eq. (29), the said system reduces to an eigen value problem for the vibration frequency ω.

Interpretation

In the postbuckling state, the variation of the nondimensional natural frequencies around the first buckled configuration versus the fluid velocity, the fluid density and the initial tension for F-F is plotted in Figs. 8(a-c). The similar plots for F-H and H-H FG pipes are exhibited by Figs. 9(a-c) and 10(a-c), respectively.

For F-F pipe, in the postbuckling domain, the first and the third natural frequencies increase with the control parameters while the second frequency remains constant. For F-H pipe, a rapid increase of the natural frequencies is shown for low values of the control parameters. Relatively high values of control parameters have no significant influence on the natural frequencies. It can be easily seen in Fig. 10 that for H-H pipe, just the natural frequency corresponding to the fist vibration mode is a function of control parameters. The Second and the third natural frequencies are independent of the studied parameters.

7. Conclusion

In this paper, buckling and post-buckling behavior of fluid conveying FG pipe is investigated. First, the buckling configuration of the FG pipe with different boundary conditions was derived. It is shown that for the selected boundary conditions, the transverse displacement is proportional to the power-law index. On the contrary, the critical values of the control

parameters decreased with increasing the power-law index. The critical values corresponding to the F-F supports are the most amongst the three boundary conditions which illustrate the high stability of a pipe having this kind of supports. It was also highlighted that the FG pipe deflection increases as the control parameters increase. The linear vibrations in the proximity of the first buckled configuration are studied and a closed form solution for the natural frequencies and their associated mode shapes is derived. The three lowest natural frequencies are obtained for Fluid conveying FG pipe with different boundary conditions. It has been clarified that the impact of the control parameters on the first natural frequencies depends on the boundary conditions.

Declarations

Competing interests: The author declare that they have no known competing financial interests or personal relationships that could have appeared to influence the work reported in this paper.

Funding: Not applicable

Authors' contributions: The whole work is done by a single author

Acknowledgements: Not applicable

Authors' information: Dr. Abdellatif Selmi. Prince Sattam bin Abdulaziz University, College of Engineering, Civil Engineering Department, Alkharj 11642, Saudi Arabia

Email: Selmi_fr2016@yahoo.com

References

[1] Paidoussis, M.P.: Fluid-Structure Interactions: Slender Structures and Axial Flow, vol. 1. Academic Press, London (2014)

[2] Ibrahim, R.A.: Mechanics of pipes conveying fluids–Part II: applications and fluid elastic problems. J. Press. Vessel Technol. 133, 24001 (2011)

[3] Modarres-Sadeghi, Y., Paidoussis, M.P.: Nonlinear dynamics of extensible fluid-conveying pipes, supported at both ends. J. Fluids Struct. 25, 535–543 (2009)

[4] Wang, L., Dai, H.L., Qian, Q.: Dynamics of simply supported fluid-conveying pipes with geometric imperfections. J. Fluids Struct. 29, 97–106 (2012)

[5] Dai, H.L., Wang, L., Qian, Q., Ni, Q.: Vortex-induced vibrations of pipes conveying pulsating fluid. Ocean Eng. 77, 12–22 (2014)

[6] Wang, L., Dai, H.L.M: Vibration and enhanced stability properties of fluid-conveying pipes with two symmetric elbows fitted at downstream end. Arch. Appl. Mech. 82,155–61 (2012)

[7] Łuczko, J., Czerwiński, A.: Nonlinear three-dimensional dynamics of flexible pipes conveying fluids. J. Fluid Struct. 70, 235–60 (2017)

[8] Ghayesh, M.H., Païdoussis, M.P., Modarres-Sadeghi, Y.: Three-dimensional dynamics of a fluid-conveying cantilevered pipe fitted with an additional spring-support and an end-mass. J. Sound Vib. 330, 2869–99 (2011)

[9] Paidoussis, M.P., Issid, N.T.: Dynamic stability of pipes conveying fluid. J. Sound Vib. 33, 267–94 (1974)

[10] An, C., Su, J.: Dynamic behavior of pipes conveying gas liquid two-phase flow. Nucl. Eng. Des. 292, 204–212 (2015)

[11] Dai, H.L., Wang, L., Ni, Q.: Dynamics of a fluid-conveying pipe composed of two different materials. Int. J. Eng. Sci. 73, 67–76 (2013)

[12] Sadeghi, M.H., Karimi-Dona, M.H.: Dynamic behavior of a fluid conveying pipe subjected to a moving sprung mass–an FEM-state space approach. Int. J. Pressure Vessels Pip. 88, 123–31 (2011)

[13] Wang, L., Dai, H.L., Ni, Q.: Nonconservative pipes conveying fluid: evolution of mode shapes with increasing flow velocity. J. Vib. Control 21, 3359–3367 (2015)

[14] Wang, L., Dai, H.L., Ni. Q.: Mode exchange and unstable modes in the dynamics of conical pipes conveying fluid. J. Vib. Control 22, 1003–1009 (2016)

[15] Yang, X.D., Yang, T.Z., Jin, J.D.: Dynamic stability of a beam-model viscoelastic pipe for conveying pulsative fluid. Acta. Mech. Solid Sin. 20, 350–356 (2007)

[16] Panda, L.N., Kar, R.C.: Nonlinear dynamics of a pipe conveying pulsating fluid with combination, principal parametric and internal resonances. J. Sound Vib. 309, 375–406 (2008)

[17] Seo, Y.S., Jeong, W.B., Jeong, S.H., Oh, J.S., Yoo, W.S.: Finite element analysis of forced vibration for a pipe conveying harmonically pulsating fluid. Int. J. C. Mech. Syst. 48, 688–694 (2005)

[18] Zhai, H., Wu, Z., Liu, Y., Yue, Z.: In-plane dynamic response analysis of curved pipe conveying fluid subjected to random excitation. Nucl. Eng. Des. 256, 214–226 (2013)

[19] Qian, Q., Wang, L., Ni, Q.: Instability of simply supported pipes conveying fluid under thermal loads. Mech. Res. Commun. 36(3), 413–7 (2009)

[20] Chang, G.H., Modarres-Sadeghi, Y.: Flow-induced oscillations of a cantilevered pipe conveying fluid with base excitation. J. Sound Vib. 333, 4265–4280 (2014)

[21] Paidoussis, M.P., Issid, N.T.: Dynamic stability of pipes conveying fluid. J. Sound Vib. 33, 267–294 (1974)

[22] Ariaratnam, S.T., Namachchivaya, N.S.: Dynamic stability of pipes conveying pulsating fluid. J. Sound Vib. 107, 215–230 (1986)

[23] Yoshizawa, M., Nao, H., Hasega, E., Tsujioka, Y.: Lateral vibration of a flexible pipe conveying fluid with pulsating flow. Bull. JSME. 29, 2243–2250 (1986)

[24] Namchchivaya, N.S.: Non-linear dynamics of supported pipe conveying pulsating fluid-I. Subharmonic resonance. Int. J. Non Linear Mech. 24, 185–196 (1989)

[25] Sri Namchchivaya, N., Tien, W.M.: Non-linear dynamics of supported pipe conveying pulsating fluid-II. Combination resonance. Int. J. Non Linear Mech. 24, 197–208 (1989)

[26] Jin, J.D., Song, Z.Y.: Parametric resonances of supported pipes conveying pulsating fluid. J. Fluids Struct. 20, 763–783 (2005)

[27] Askarian, A.R., Haddadpour, H., Firouz-Abadi, R.D., Abtahi, H.: Nonlinear dynamics of extensible viscoelastic cantilevered pipes conveying pulsatile flow with an end nozzle. Int. J. Non Linear Mech. 91, 22–35 (2017)

[28] Czerwinski, A., Łuczko, J.: Parametric vibrations of flexible hoses excited by a pulsating fluid flow, Part II: experimental research. J. Fluids Struct. 55, 174–190 (2015)

[29] Łuczko, J., Czerwinski, A.: Parametric vibrations of flexible hoses excited by a pulsating fluid flow, Part I: modelling, solution method and simulation. J. Fluids Struct. 55, 155–173 (2015)

[30] Li, Y., Yang, Y.: Nonlinear vibration of slightly curved pipe with conveying pulsating fluid. Nonlinear Dyn. 88, 2513–2529 (2017)

[31] Hiramoto, K., Doki, H.: Simultaneous optimal design of structural and control systems for cantilevered pipes conveying fluid. J. Sound Vib. 274, 685–99 (2004)

[32] Doki, H., Hiramoto, K., Skelton, R.E.: Active control of cantilevered pipes conveying fluid with constraints on input energy. J. Fluid Struct. 12, 615–28 (1998)

[33] Qian, Q., Wang, L., Ni, Q.: Instability of simply supported pipes conveying fluid under thermal loads. Mech. Res. Commun. 36, 413–417 (2009)

[34] Koizumi, M.: The concept of FGM. Ceram. Trans. Funct. Gradient Mater. 34, 3–10 (1993)

[35] Fuchiyama, T., Noda, N.: Analysis of thermal stress in a plate of functionally gradient material. JSAE Rev. 16, 263–268 (1995)

[36] Hosseini, M., Fazelzadeh, S.A.: Thermomechanical stability analysis of functionally graded thin-walled cantilever pipe with flowing fluid subjected to axial load. Int. J. Struct. Stab. Dyn. 11, 513–534 (2011)

[37] Eftekhari, M., Hosseini, M.: On the stability of spinning functionally graded cantilevered pipes subjected to fluid thermomechanical loading. Int. J. Struct. Stab. Dyn. 16, 1550062 (2016)

[38] Deng, J., Liu, Y., Zhang, Z., Liu,W.: Stability analysis of multi-span viscoelastic functionally graded material pipes conveying fluid using a hybrid method. Eur. J. Mech. A-Solid 65, 257–70 (2017)

[39] Wang, Z.M., Liu, Y.Z.: Transverse vibration of pipe conveying fluid made of functionally graded materials using a symplectic method. Nucl. Eng. Des. 298, 149–59 (2016)

[40] An, C., Su, J.: Dynamic Behavior of Axially Functionally Graded Pipes Conveying Fluid. Math. Probl. Eng. 2017, 1–11 (2017)

[41] Nayfeh, A.H., Emam, S.A.: Exact solutions and stability of the postbuckling configurations of beams. Nonlinear Dyn. 54, 395–408 (2008)

.

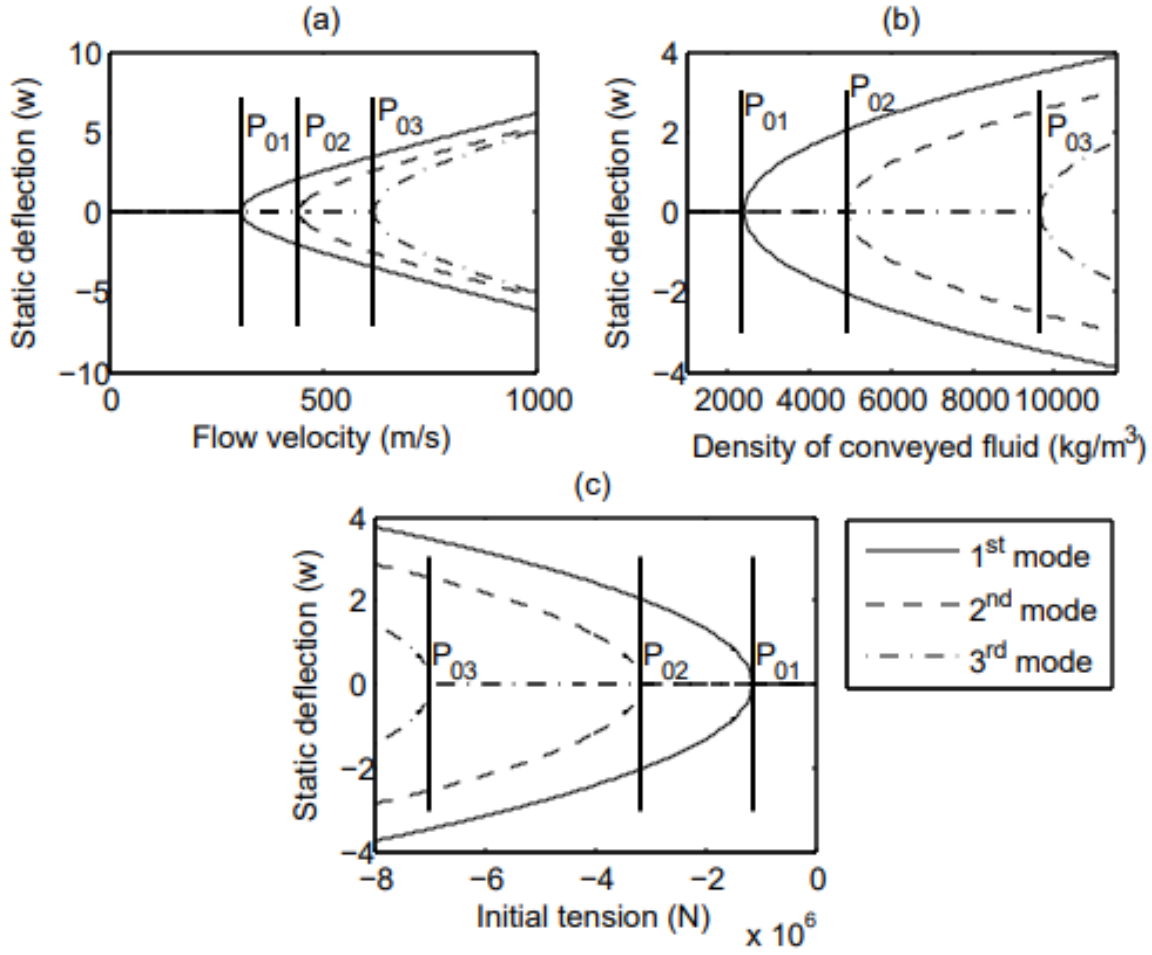

Fig. 2. Bifurcation diagram for the static deflection of a F-F FG pipe conveying fluid at x=0.25 with the (a) flow velocity, (b) fluid density and (c) initial tension

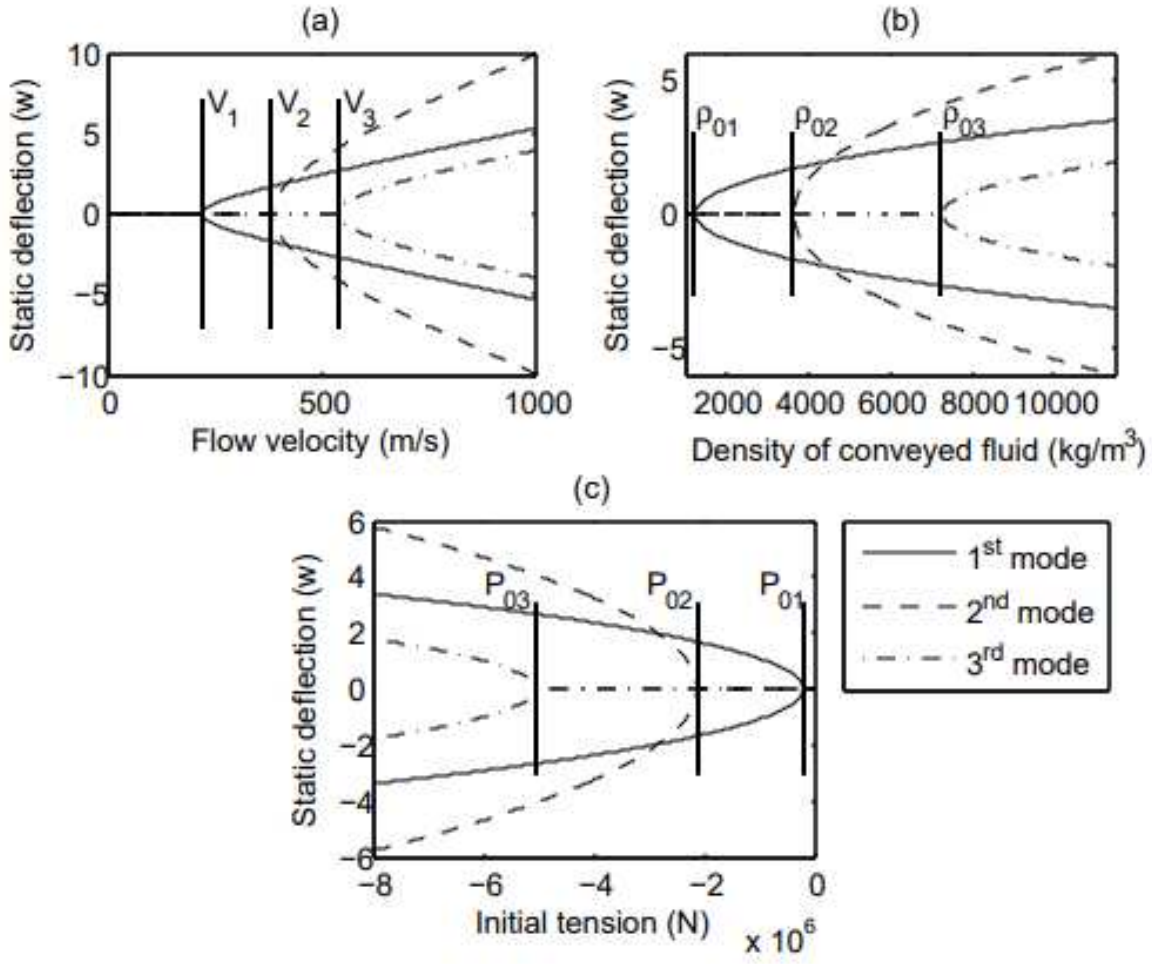

Fig. 3. Bifurcation diagram for the static deflection of a F-H FG pipe conveying fluid at x=0.25 with the (a) flow velocity, (b) fluid density and (c) initial tension

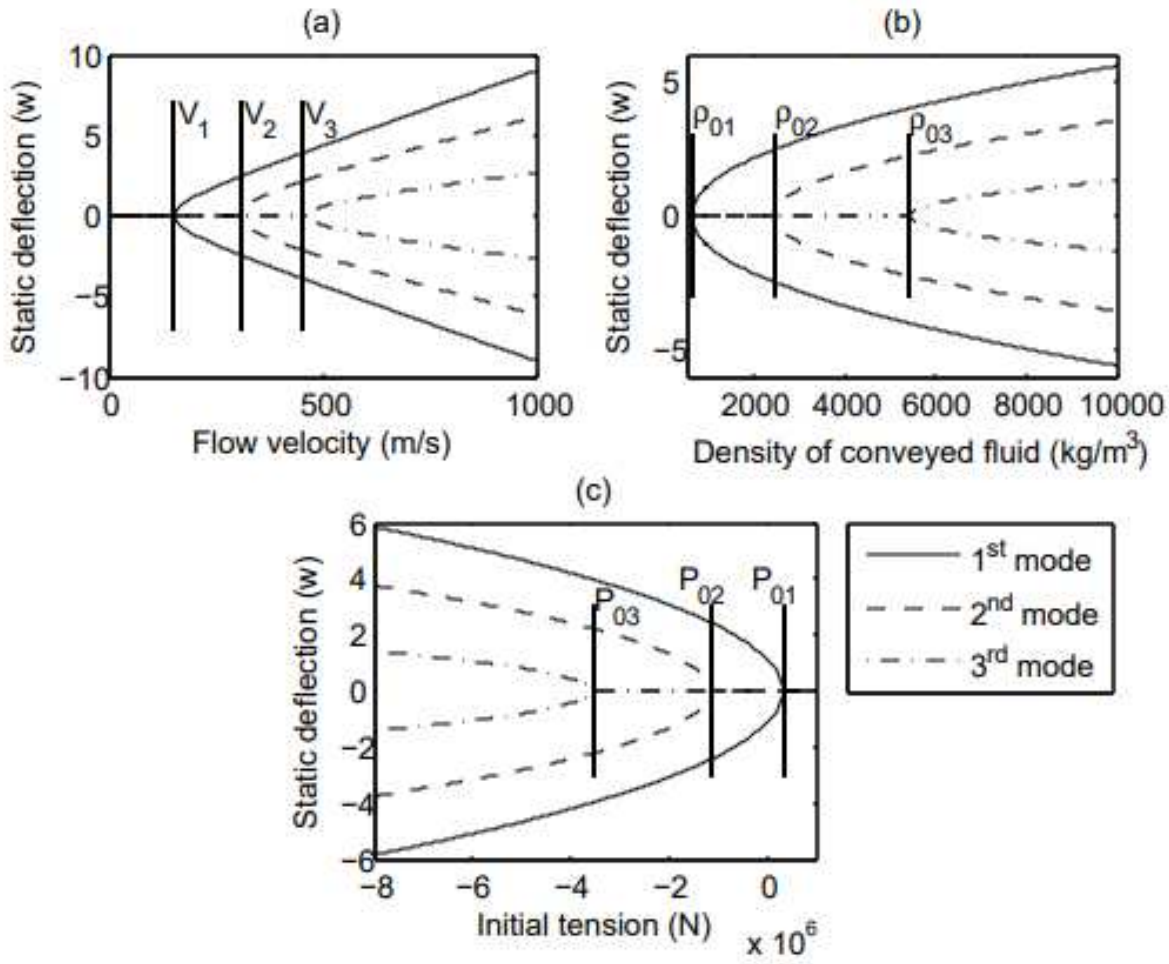

Fig. 4. Bifurcation diagram for the static deflection of a H-H FG pipe conveying fluid at x=0.25 with the (a) flow velocity, (b) fluid density and (c) initial tension

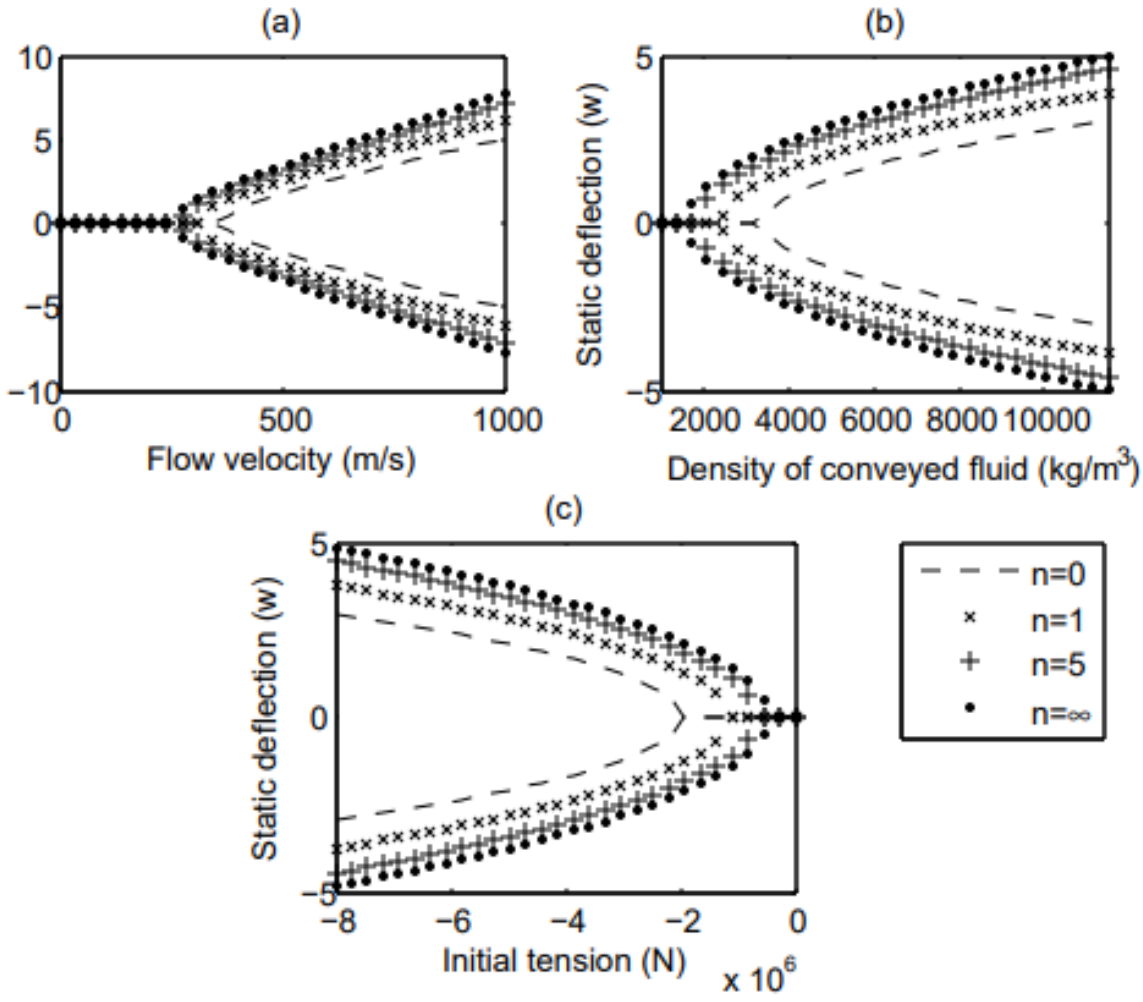

Fig. 5. Bifurcation diagram for the static deflection of a F-F FG pipe conveying fluid at x=0.25 with the (a) flow velocity, (b) fluid density and (c) initial tension for different values of power law index

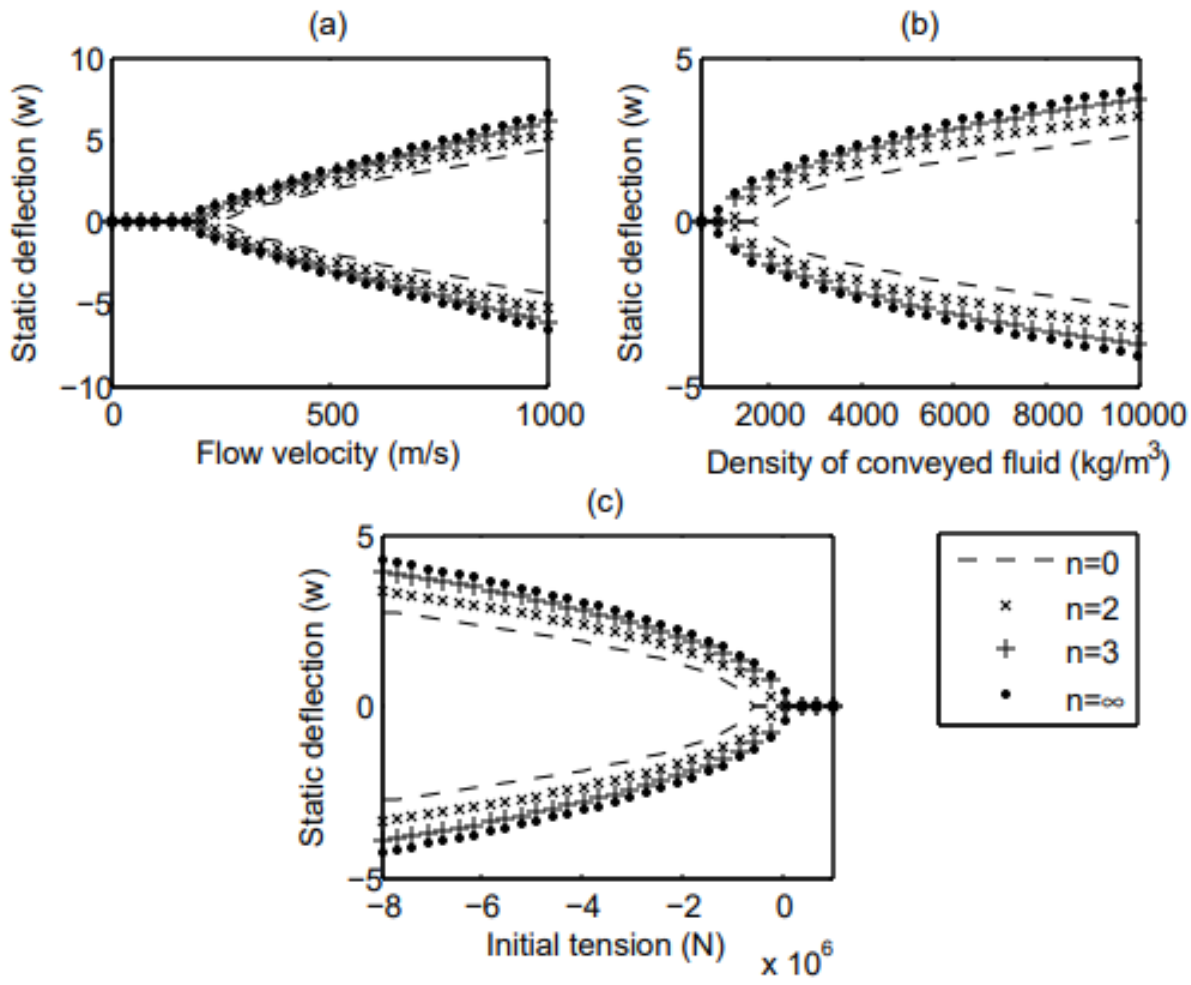

Fig. 6. Bifurcation diagram for the static deflection of a F-H FG pipe conveying fluid at x=0.25 with the (a) flow velocity, (b) fluid density and (c) initial tension for different values of power law index

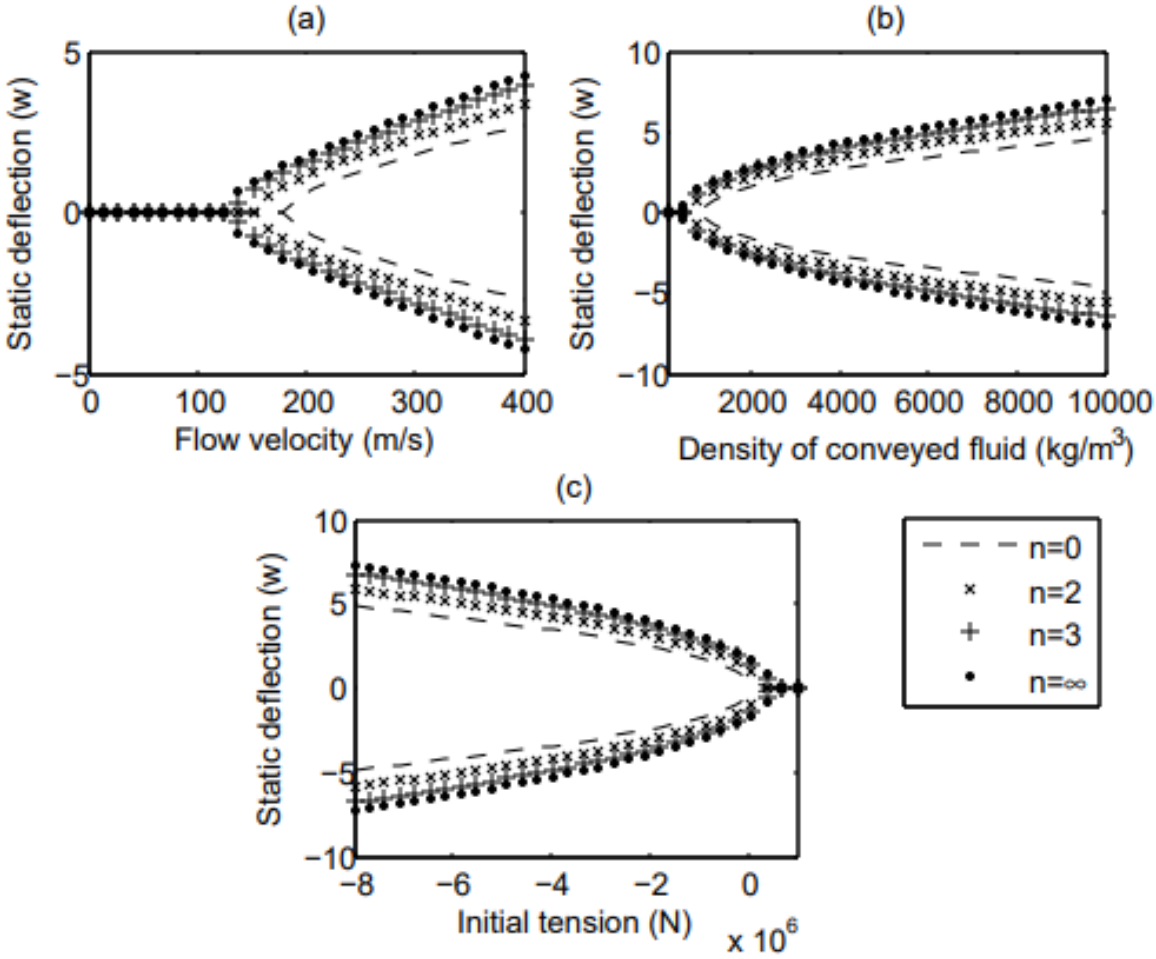

Fig. 7. Bifurcation diagram for the static deflection of a H-H FG pipe conveying fluid at x=0.25 with the (a) flow velocity, (b) fluid density and (c) initial tension for different values of power law index

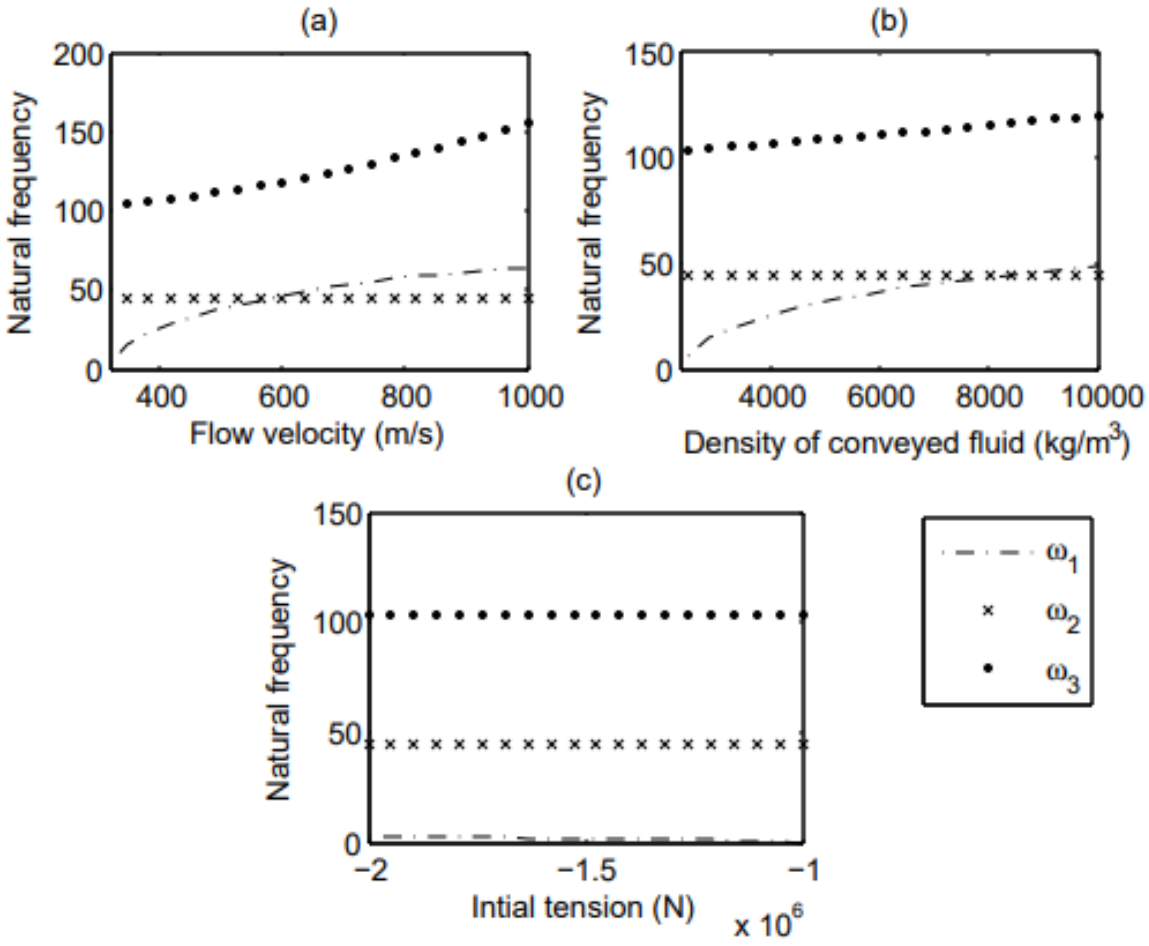

Fig. 8. Variation of the natural frequencies of vibration around the lowest three buckled configurations of a F-F FG pipe conveying fluid

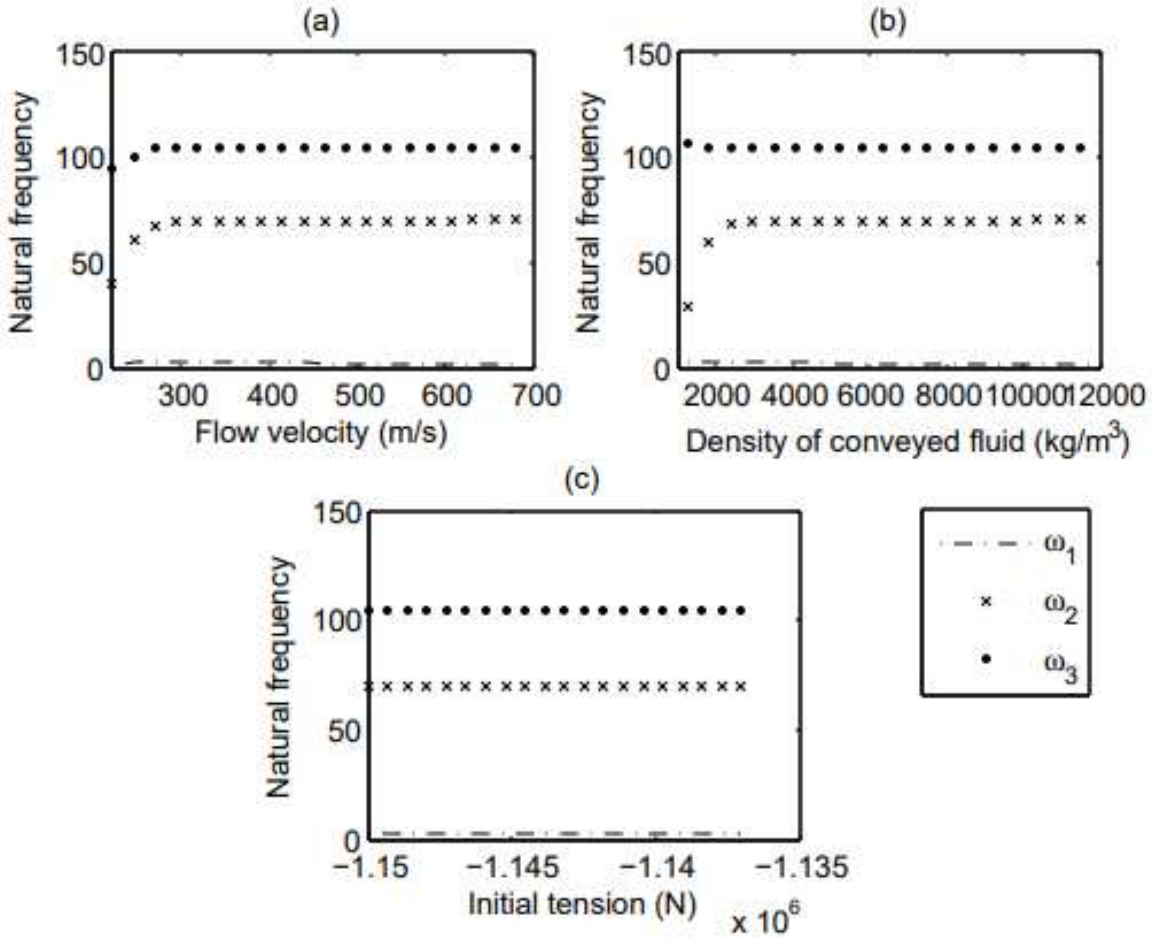

Fig. 9. Variation of the natural frequencies of vibration around the lowest three buckled configurations of a F-H FG pipe conveying fluid

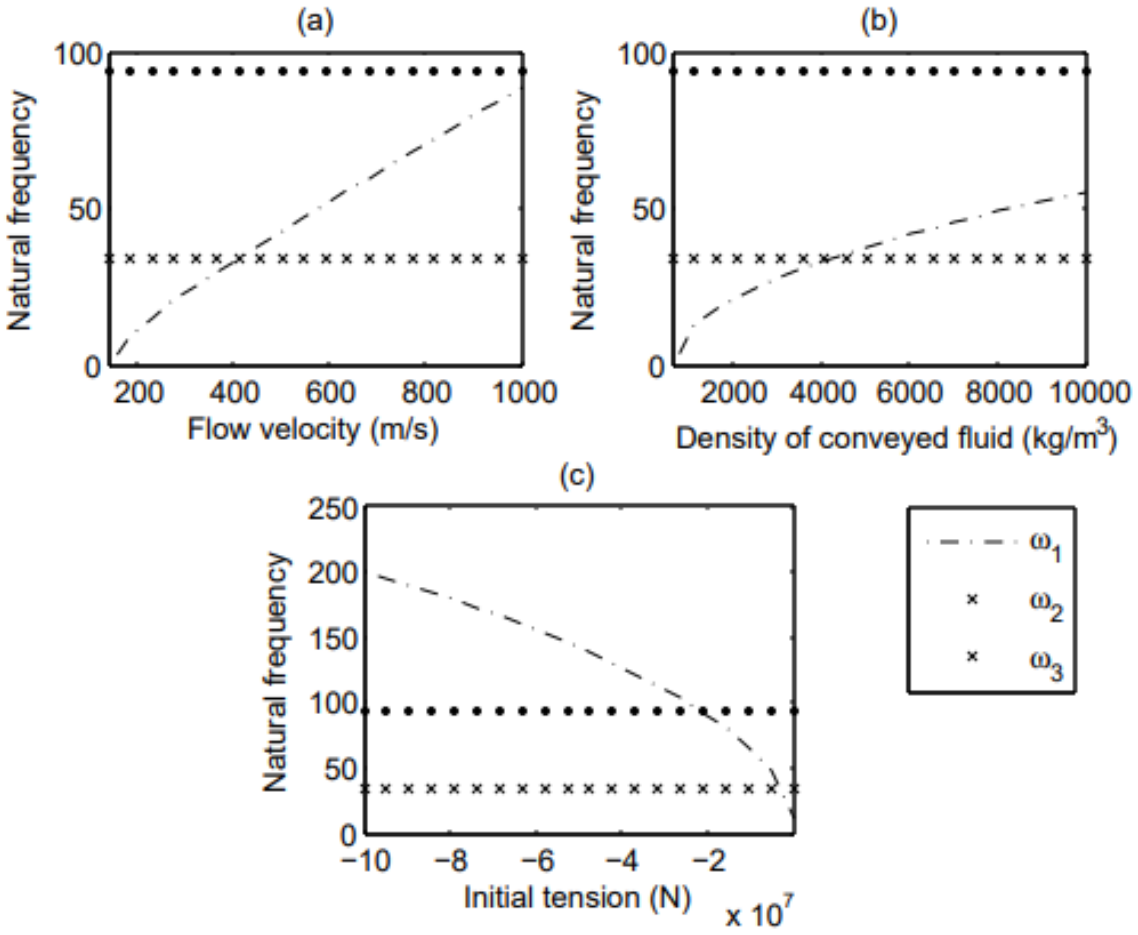

Fig. 10. Variation of the natural frequencies of vibration around the lowest three buckled configurations of a H-H FG pipe conveying fluid

Figures

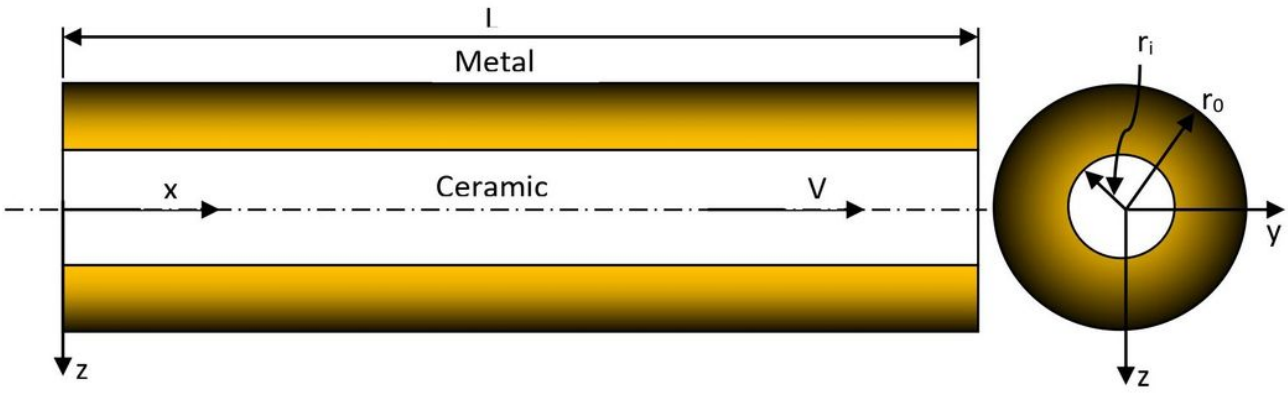

Figure 1

Schematic representation of a FG pipe conveying fluid

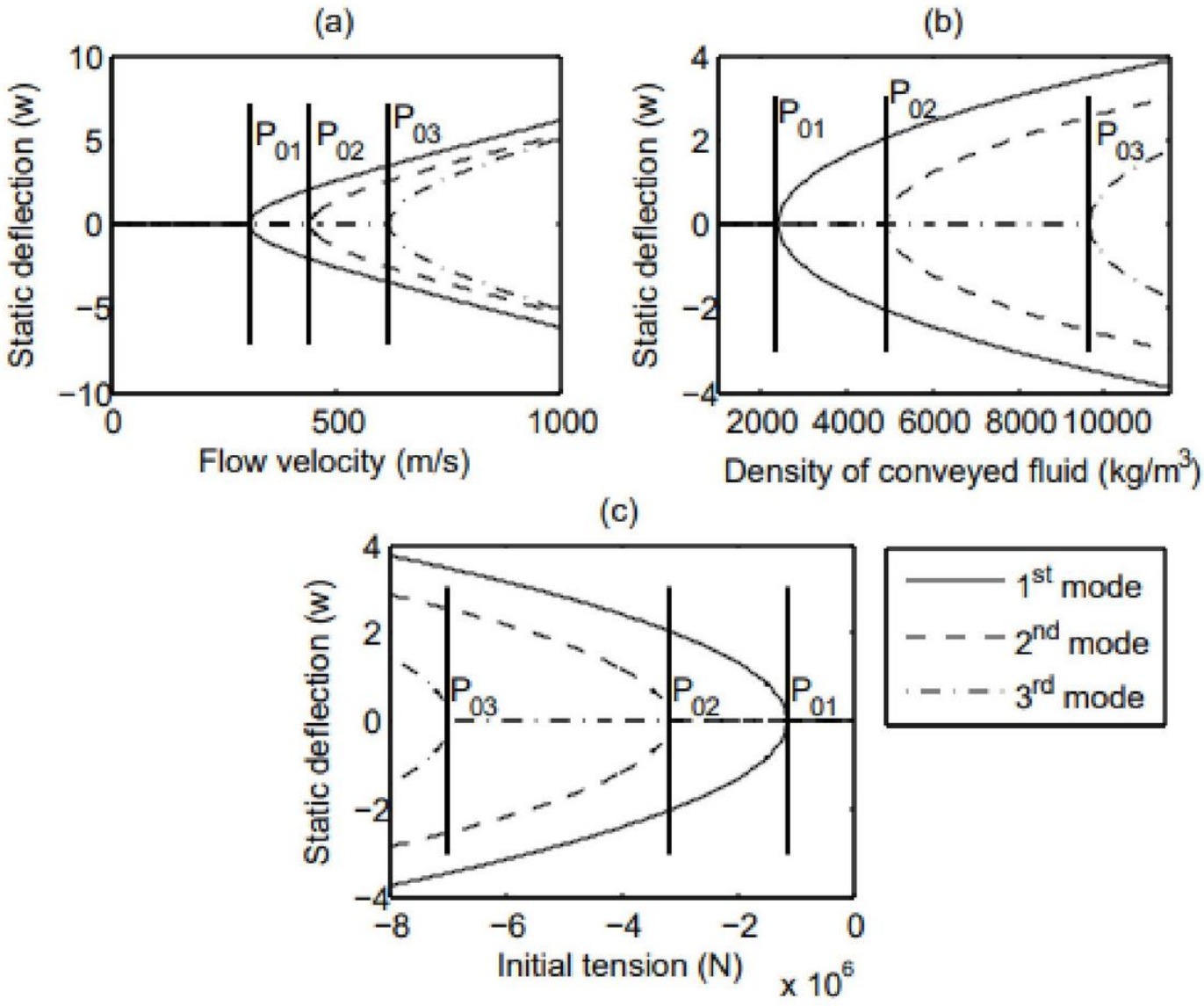

Figure 2

Bifurcation diagram for the static deflection of a F-F FG pipe conveying fluid at x=0.25 with the (a) flow velocity, (b) fluid density and (c) initial tension

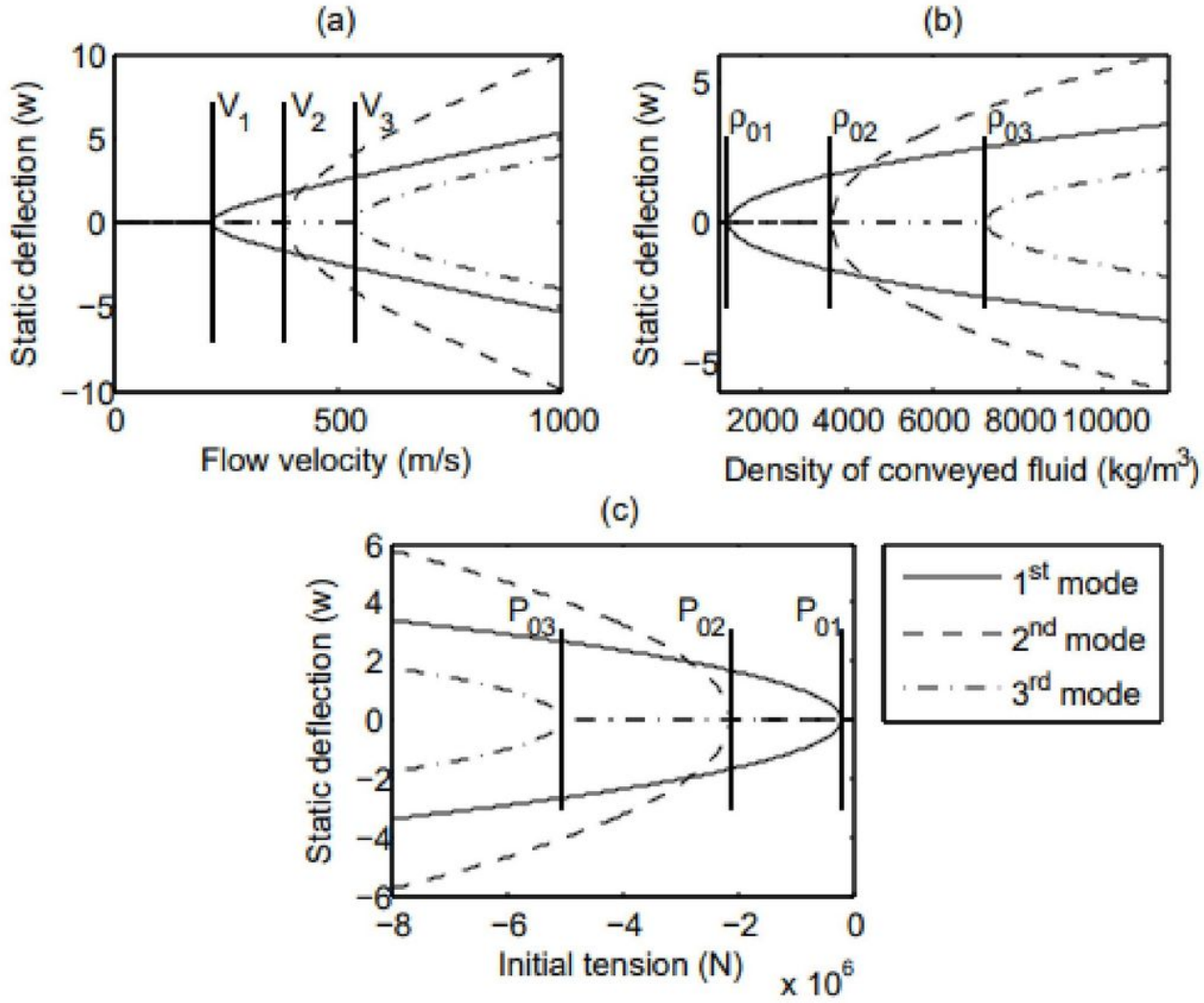

Figure 3

Bifurcation diagram for the static deflection of a F-H FG pipe conveying fluid at x=0.25 with the (a) flow velocity, (b) fluid density and (c) initial tension

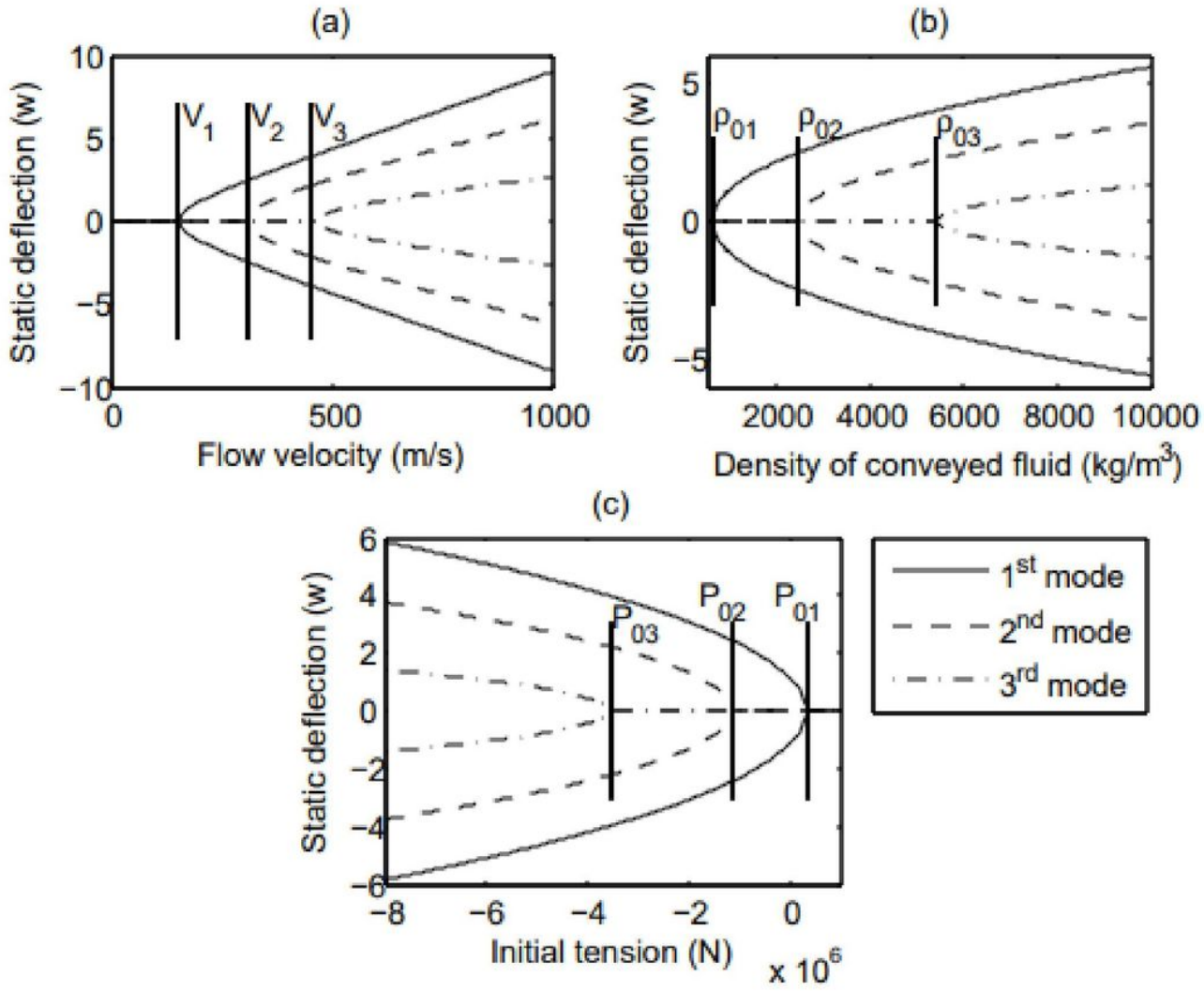

Figure 4

Bifurcation diagram for the static deflection of a H-H FG pipe conveying fluid at x=0.25 with the (a) flow velocity, (b) fluid density and (c) initial tension

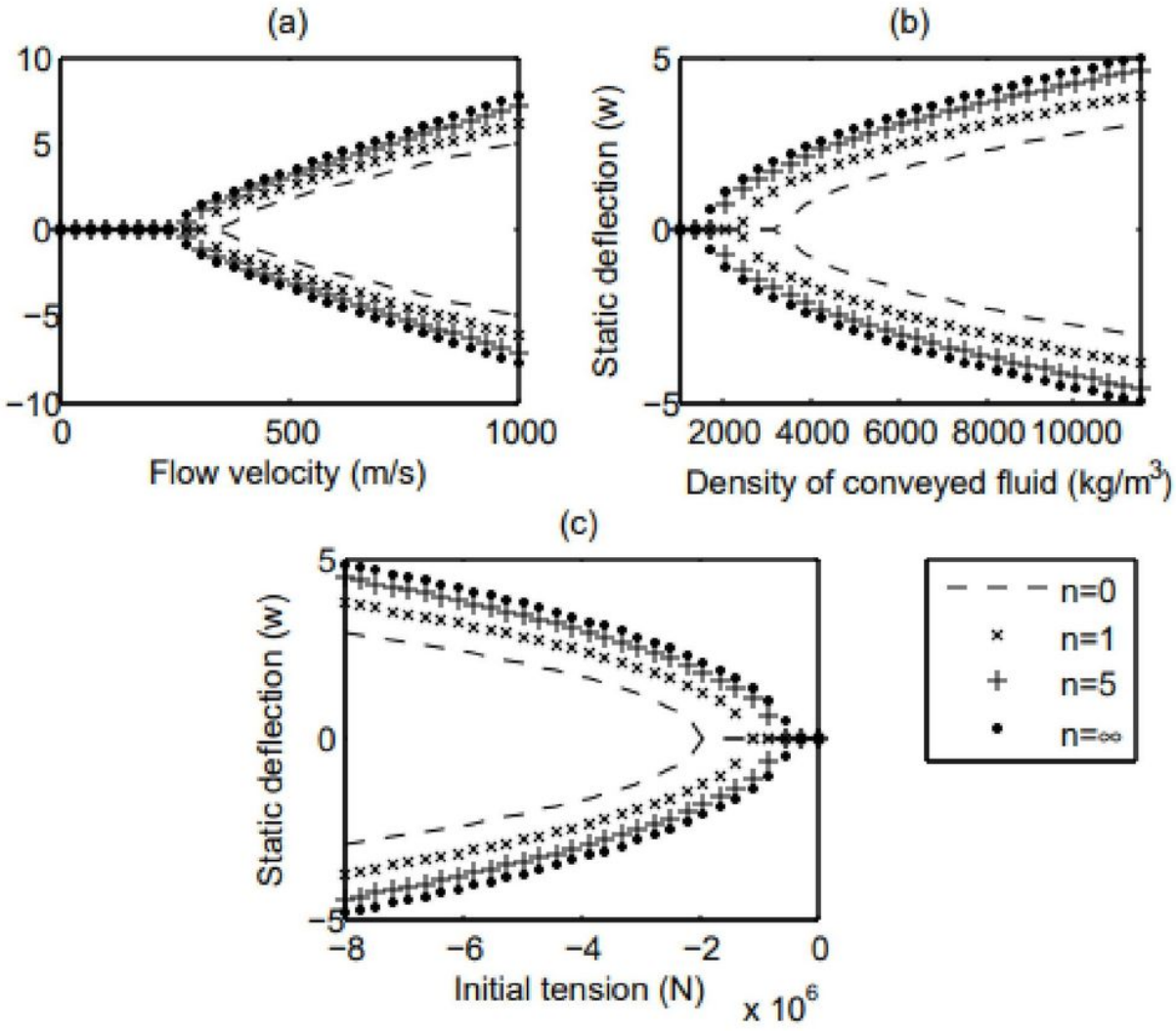

Figure 5

Bifurcation diagram for the static deflection of a F-F FG pipe conveying fluid at x=0.25 with the (a) flow velocity, (b) fluid density and (c) initial tension for different values of power law index

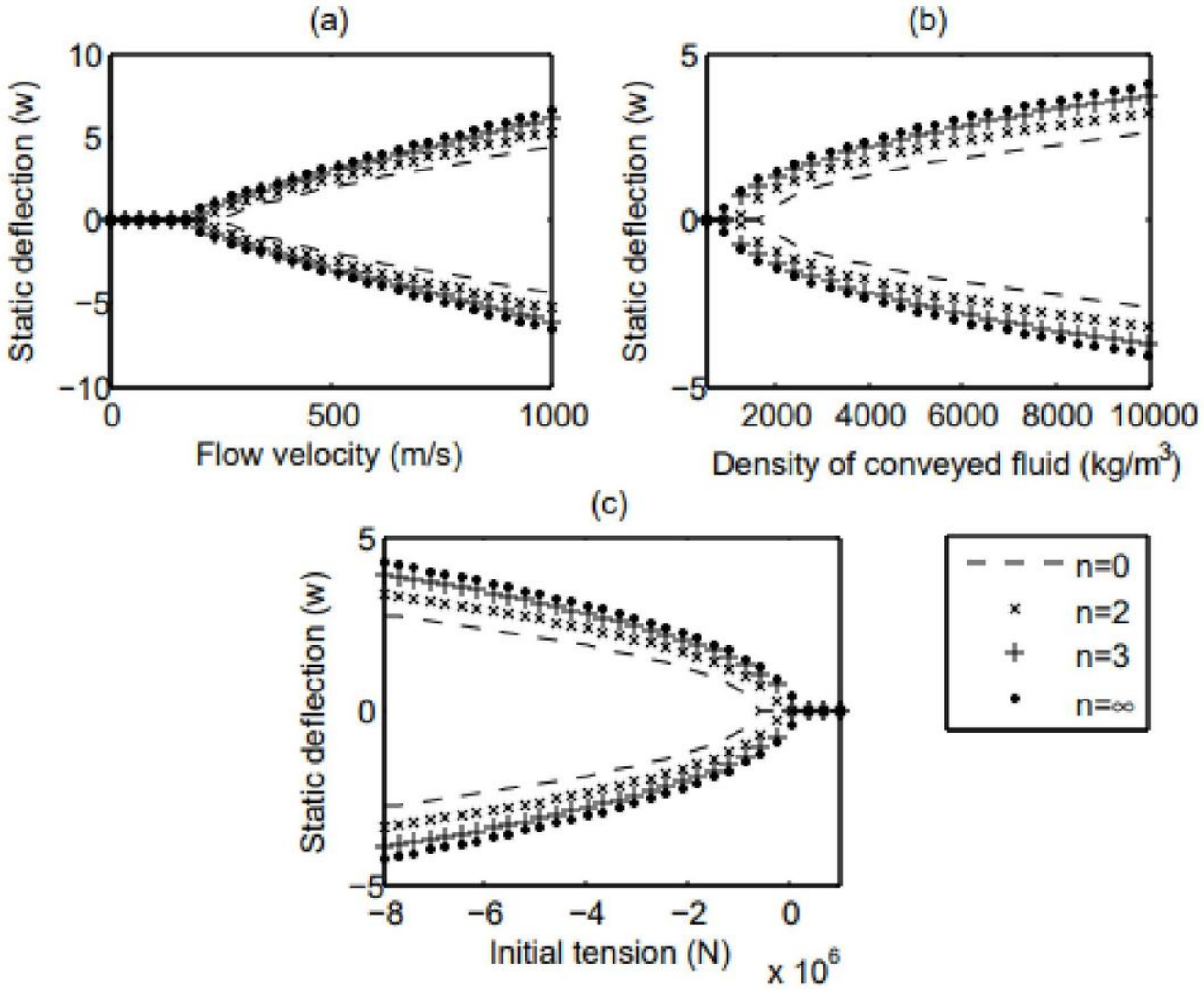

Figure 6

Bifurcation diagram for the static deflection of a F-H FG pipe conveying fluid at x=0.25 with the (a) flow velocity, (b) fluid density and (c) initial tension for different values of power law index

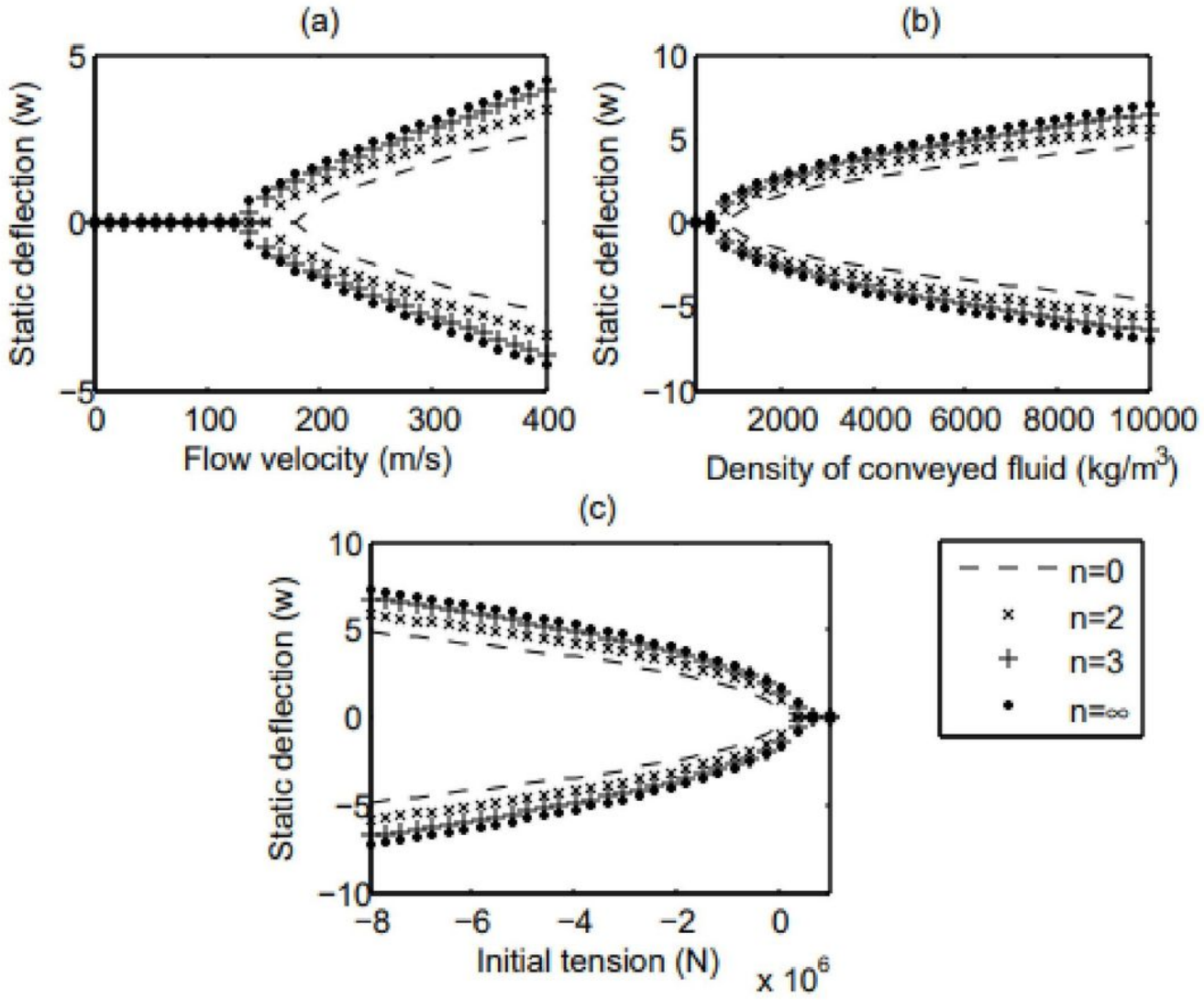

Figure 7

Bifurcation diagram for the static deflection of a H-H FG pipe conveying fluid at x=0.25 with the (a) flow velocity, (b) fluid density and (c) initial tension for different values of power law index

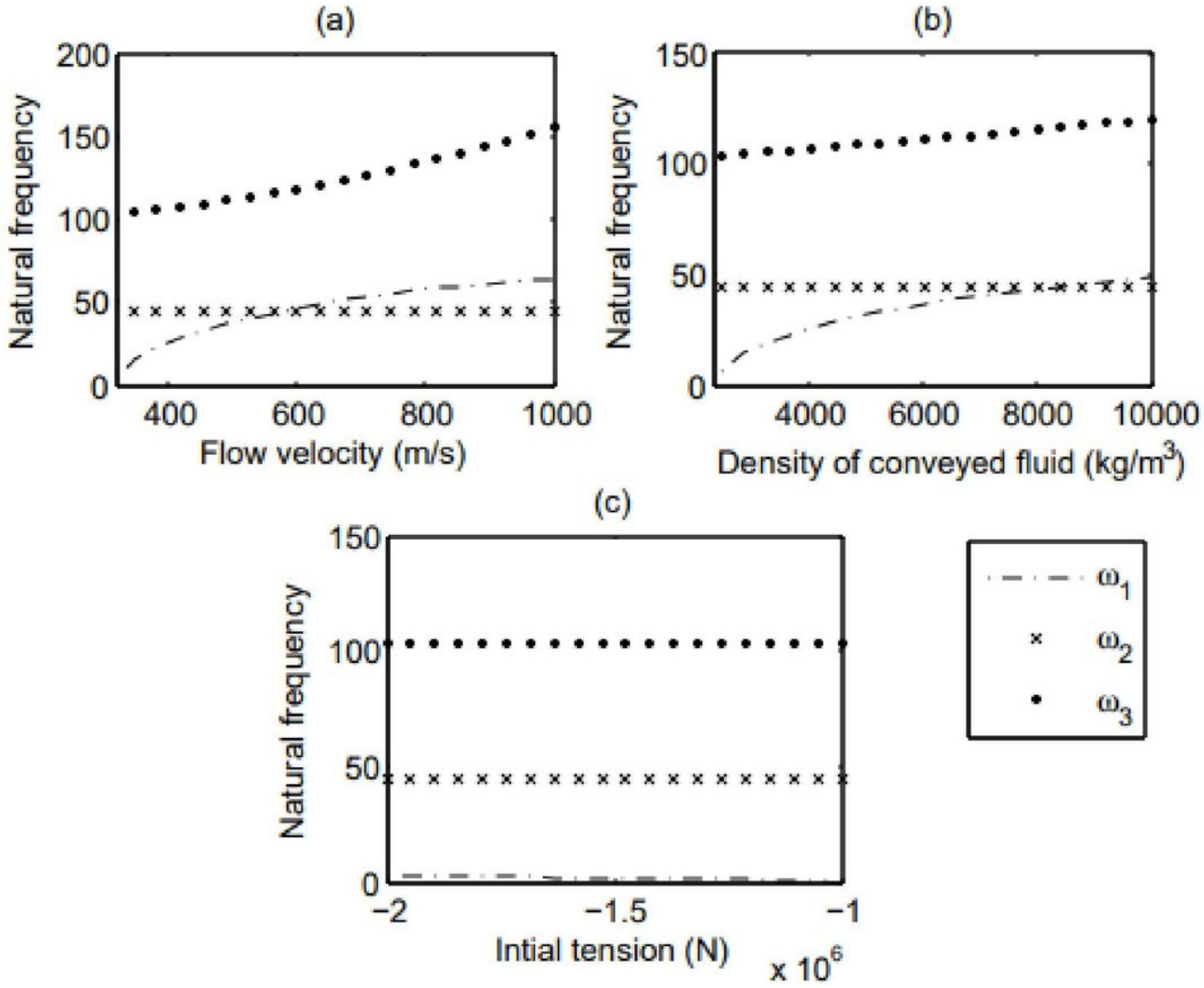

Figure 8

Variation of the natural frequencies of vibration around the lowest three buckled configurations of a F-F FG pipe conveying fluid

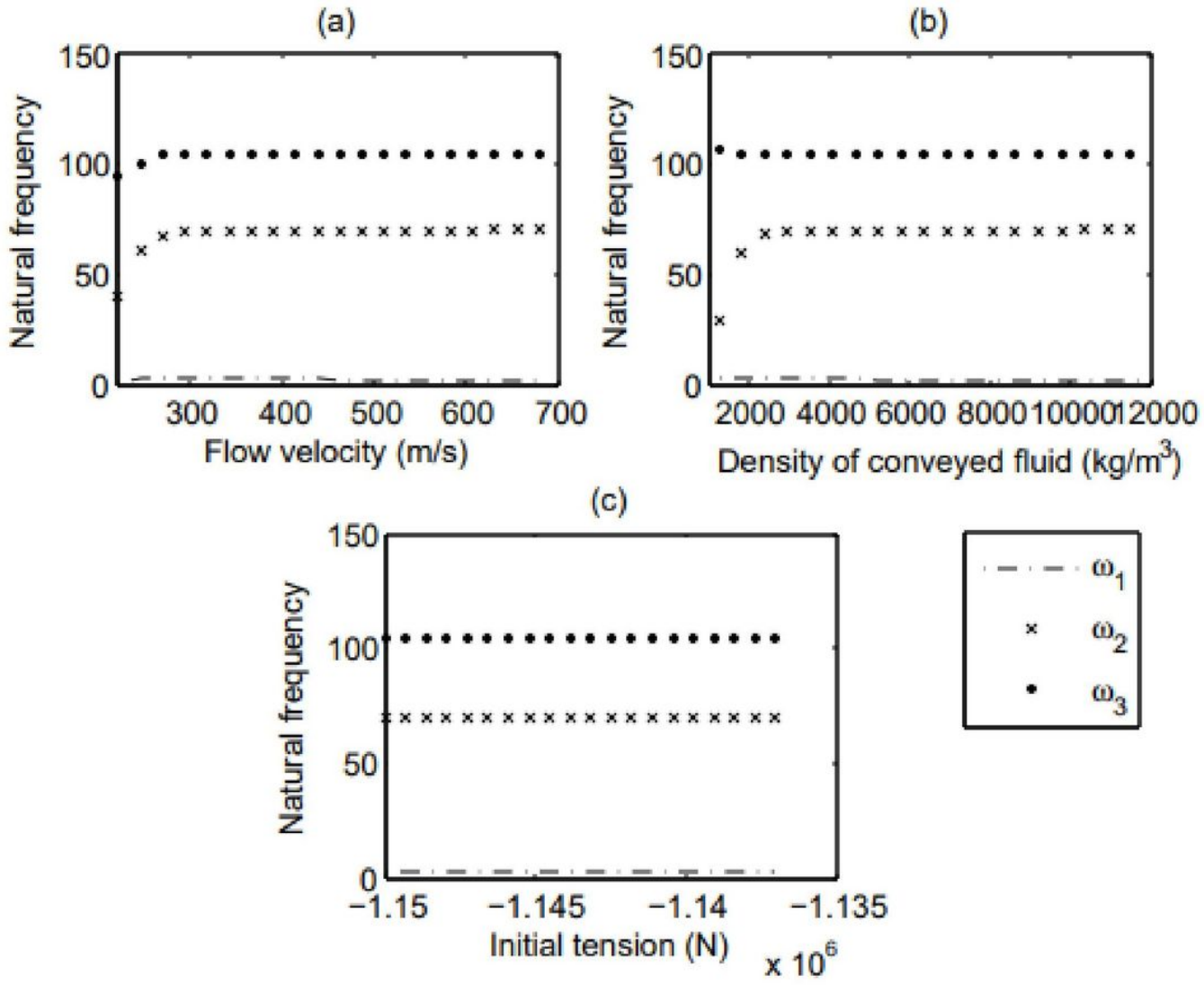

Figure 9

Variation of the natural frequencies of vibration around the lowest three buckled configurations of a F-H FG pipe conveying fluid

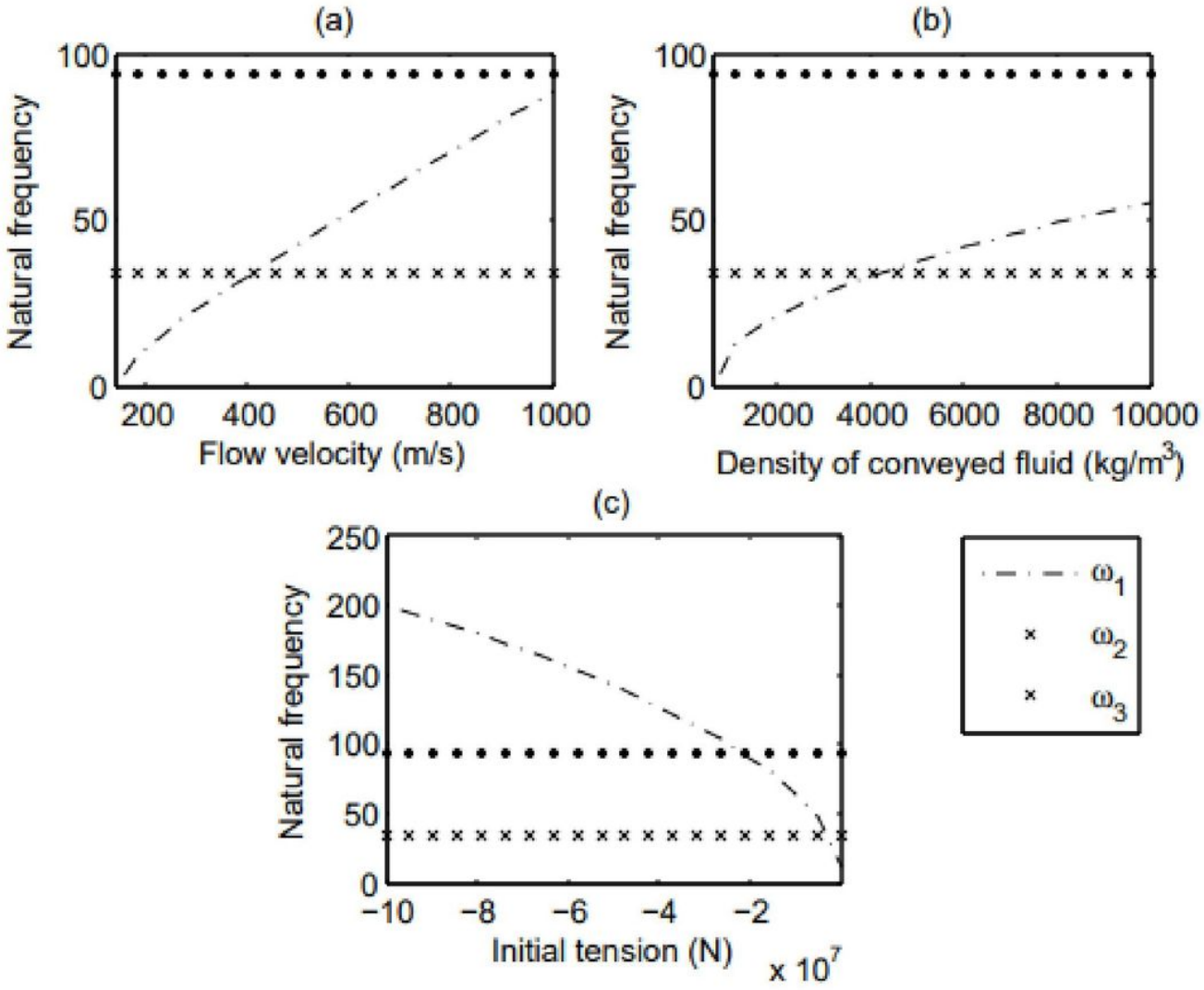

Figure 10

Variation of the natural frequencies of vibration around the lowest three buckled configurations of a H-H FG pipe conveying fluid